厚生労働科学研究費補助金　（障害者対策総合研究事業（神経・筋疾患分野））
「異常タンパク伝播仮説に基づく神経疾患の画期的治療法の開発」
（分担）研究報告書

ALSではいつ細胞障害が始まるのか？TDP-43陽性封入体との関係

研究分担者：氏名小野寺理[1)]
研究協力者：須貝章弘[2)]、小山哲秀[3)]、加藤泰介[2)]、志賀篤[3)]、今野卓哉[2)]
小山美咲[2)]、石原智彦[1)]、西澤正豊[2)]
1）新潟大学脳研究所分子神経疾患資源解析学分野
2）新潟大学脳研究所神経内科
3）新潟大学研究推進機構超域学術院
4）新潟大学脳研究所病理学分野

研究要旨 孤発性ALSではTDP-43の核からの消失と細胞質内での不入対の形成が特徴的である．TDP-43遺伝子変異をもつ家族性ALSの存在はTDP-43の異常が一次的な意義を持つことを示している．しかし，TDP-43病理が一次的な意義を持つのかどうかは明らかではない．我々は，ALSの運動神経細胞にて，核内小体であるGEM小体の数が減少していること．TDP-43 mRNAの細胞内局在が変化していることを見出した．ALSで見られるTDP-43病理と，これらの所見を比較した結果，GEM小体の減少は，TDP-43病理の出現に先行することを示した．

A.研究目的

TDP-43変異による筋萎縮性側索硬化症（ALS）の存在は、TDP-43がALSの病態に一次的な意義を持つことを明確に示している。孤発性、およびTDP-43変異を伴うALSでは、罹患部位の残存神経細胞に、TDP-43陽性の細胞内封入体と、核蛋白であるTDP-43の核からの消失を認める。しかし、この病理学的なTDP-43の異常と細胞障害性との関連は未だ十分に明らかにはされていない。

ALS運動神経細胞にてTDP-43に関連して生じている変化として，我々は3つの事を明らかとしてきた．一つはTDP-43の消失によるTDP-43の機能であるスプライシングの異常，POLDIP3のスプライシング異常である．もう一つは，TDP-43が核内小体であるGEMに局在することから推察した，GEM小体の減少と，それに伴うUsnRNAの異常である．この現象は，脊髄性筋萎縮症でも認められ，さらに同様にALSを引き起こすFused sarcoma 遺伝子異常を伴うALSにても指摘された．これらの事実は，この現象が，　運動神経細胞死に特異的な現象である可能性を示唆する．最後は，TDP-43の自己蛋白量制御機構に伴う，細胞内のRNA局在変化である．TDP-43は、正常細胞において一

定量に制御される。我々はこれまでに、TDP-43の増加時には、TDP-43がpolyA 選択性を変化させ、一部を核内に保存し，さらに複数のスプライシングを惹起することにより、ナンセンス依存性mRNA分解機構（NMD）を介し自己mRNAの分解を引き起こす。一方TDP-43減少時は，産生されたmRNAは速やかに細胞質に移動し，核内のTDP-43 mRNAの現象と細胞質内での増加を引き起こす.

これらの異常は何れもTDP-43の機能に注目して検討された物である．もしALSでの運動神経細胞機能障害が，TDP-43の核内からの消失，細胞質で封入体形成によるのであれば，これらの異常はTDP-43が核外に移動した細胞のみで認められるはずである．本研究では，この3点について，TDP-43の核への局在の有無により検討を加えた.

B.研究方法

孤発性ALS患者の脊髄前核運動神経細胞を、TDP-43の封入体の有無、核内TDP-43の有無により分け、TDP-43が関連する①核内のGEM小体の数　②TDP-43 mRNAの細胞内局在の変化を免疫蛍光染色法にて比較検討した。

C.研究結果

我々は、ALS患者の残存脊髄前核細胞にて、GEM小体の数が減少すること、TDP-43 mRNAの細胞内局在が変化することを明らかとしてきた。これらの変化がTDP-43陽性の細胞質内封入体の有無により異なるかを比較した。その結果、TDP-43陽性封入体の有無にかかわらず、核内のGEM小体は減少した。一方TDP-43 mRNAの細胞内局在はTDP-43細胞質内封入体を認める物で有意に異常を示した。この事実は、免疫組織化学的にTDP-43の核外移動が認められない細胞でも、すでに細胞障害が生じている可能性を示唆する。一方TDP-43 mRNAの細胞内局在の異常は核からのTDP-43の移動に密接に関係することを示唆する。

D.考察

TDP-43が関連するALSの細胞障害性については，TDP-43の異常が先行し，TDP-43の病理学的な変化をもたらし，その細胞内局在の変化による機能喪失機序が引き起こされ，更なる変化が起こされるという仮説と，何らかの異常により，TDP-43の細胞内局在がまず変化して，その後に封入体形成や，TDP-43の機能喪失などが引き起こされるという可能性が考えられる．今回の我々の検討ではGEM小体の現象はTDP-43の核外移動に先行しており，核内のTDP-43がすでに何らかの機能異常をおこし，GEM小体の形成に影響を及ぼしている可能性を考える．GEM小体の異常は様々なpre-mRNAのスプライシングに影響を及ぼし，細胞障害性を引き起こすと考える．今回の結果からは，TDP-43病理に先行した異常がすでに起こっていて，核外移動と，細胞質内不入対の形成という病理像は，その下流である可能性を示す.

E.結論

TDP-43の免疫組織科学的な異常に先行して，TDP-43の機能異常，細胞障害が生じ

ている可能性を示唆した。

F.健康危険情報

なし

G.研究発表

（発表誌名巻号・頁・発行年等も記入）

1. 論文発表

1. 伊藤 岳, 西澤 正豊, 小野寺 理 【神経細胞変性のメカニズム】 炎症と神経変性：Brain Medical 26 巻 3 号 Page259-263(2014.10)
2. 酒井 直子, 石原 智彦, 小野寺 理, 西澤 正豊 【神経症候群(第 2 版)-その他の神経疾患を含めて-】 変性疾患 運動ニューロン疾患 筋萎縮性側索硬化症 遺伝性 ALS ALS10(TARDBP 遺伝子変異による ALS)：日本臨床(0047-1852)別冊神経症候群 II Page491-495(2014.03)
3. Akimoto C, Volk AE, van Blitterswijk M, Van den Broeck M, Leblond CS, Lumbroso S, Camu W, Neitzel B, Onodera O, van Rheenen W, Pinto S, Weber M, Smith B, Proven M, Talbot K, Keagle P, Chesi A, Ratti A, van der Zee J, Alstermark H, Birve A, Calini D, Nordin A, Tradowsky DC, Just W, Daoud H, Angerbauer S, DeJesus-Hernandez M, Konno T, Lloyd-Jani A, de Carvalho M, Mouzat K, Landers JE, Veldink JH, Silani V, Gitler AD, Shaw CE, Rouleau GA, van den Berg LH, Van Broeckhoven C, Rademakers R, Andersen PM, Kubisch C. A blinded international study on the reliability of genetic testing for GGGGCC-repeat expansions in C9orf72 reveals marked differences in results among 14 laboratories. J Med Genet. 2014 Jun;51(6):419-24.
4. Kimura T, Jiang H, Konno T, Seto M, Iwanaga K, Tsujihata M, Satoh A, Onodera O, Kakita A, Takahashi H. Bunina bodies in motor and non-motor neurons revisited: a pathological study of an ALS patient after long-term survival on a respirator. Neuropathology. 2014 Aug;34(4):392-7.

2.学会発表

1. 加藤泰介 小山哲秀 須貝章弘 豊島靖子 柿田 明美 高橋均 西澤正豊 小野寺理 筋萎縮性側索硬化症運動神経細胞における TDP-43 mRNA の細胞内局在解析 2014 年度包括脳冬のワークショップ 2014 年 12 月 東京
2. 小山哲秀 須貝章弘 今野卓哉 加藤泰介 石原智彦 西澤正豊 小野寺理 TDP-43 mRNA 量調節機構の解明 2014 年度包括脳冬のワークショップ 2014 年 12 月 東京
3. 石原智彦，柿田明美，高橋均，小野寺理，西澤正豊 Aberration of the spliceosome in amyotrophic lateral sclerosis 第 55 回日本神経学会学術大会 2014 年 5 月福岡
4. 今野卓哉 小山哲秀 逸見文昭 小山美咲 須貝章弘 加藤泰介 石原智彦 西澤正豊 小野寺理 ALS 関連 TARDBP 遺伝子変異は自身の選択

的スプライシングに影響をおよぼすか？　第55回日本神経学会学術大会　2014年5月福岡

5. 石原智彦　志賀篤　小山哲秀　柿田明美　西澤正豊　高橋均　小野寺理　ALSでのStasimonヒトホモログmRNAのスプライシング異常の検討　第55回日本神経学会学術大会　2014年5月福岡
6. 伊藤岳　小山哲秀　有泉優子　木村篤史　西澤正豊　小野寺理　TDP-43発現低下時におけるミトコンドリア・ダイナミクスの検討　第55回日本神経学会学術大会　2014年5月福岡
7. 須貝章弘　小山哲秀　加藤泰介　今野卓哉　石原智彦　西澤正豊　小野寺理　核内TDP-43減少は細胞質内TDP-43 mRNA増加をもたらす　第55回日本神経学会学術大会　2014年5月福岡
8. 須貝章弘　小山哲秀　加藤泰介　志賀篤　今野卓哉　小山美咲　石原智彦　西澤正豊　小野寺理　Coordinated autoregulation of TDP-43 and its implication for TDP-43 pathology 第55回日本神経学会学術大会　2014年5月福岡
9. Akihide Koyama, Akihiro Sugai, Taisuke Kato, Takuya Konno, Tomohiko Ishihara, Masatoyo Nishizawa, Osamu Onodera: TDP-43 is autoregulated by multiple excisions of introns in exon6 and reservation of mRNA in nucleus by TDP-43. The 37th Annual Meeting of the Japan Neuroscience Society. September 2014, Yokohama
10. Atsushi Shiga, Chigusa Kondo, Sachiko Hirokawa, Tamao Tsukie, Akinori Miyashita, Masatoyo Nishizawa, Osamu Onodera: Alternation of miRNA expression in TDP-43 depleted spinal motor neuron. The 37th Annual Meeting of the Japan Neuroscience Society. September 2014, Yokohama
11. Taisuke Kato, Akihide Koyama, Akihiro Sugai, Yasuko Toyoshima, Hitoshi Takahashi, Masatoyo Nishizawa, Osamu Onodera: Analysis of intracellular distribution of TDP-43 mRNA in affected spinal motor neuron with ALS. The 37th Annual Meeting of the Japan Neuroscience Society. September 2014, Yokohama
12. Akihiro Sugai, Taisuke Kato, Akihide Koyama, Masatoyo Nishizawa, Osamu Onodera: Endogenous TDP-43 over-expression model with disrupted auto-regulation : 10th Annual Meeting of the Oligonucleotide Therapeutics Society. October 12 – 15, 2014　Hilton San Diego Resort & Spa, San Diego, California
13. Osamu Onodera, Masatoyo Nishizawa, Hitoshi Takahashi: Update in amyotrophic lateral sclerosis: he XVIII International Congress of Neuropathology. ICN 2014, will be held in Rio de Janeiro, Brazil, in September 14-18
14. Osamu Onodera: RNA metabolism and

ALS. The 37th Annual Meeting of the Japan Neuroscience Society. September 2014, Yokohama

H.知的財産権の出願・登録状況（予定を含む）

1.特許取得

なし

2.実用新案登録

なし

3.その他

なし

ACTA NEUROPATHOLOGICA COMMUNICATIONS

RESEARCH Open Access

Pathological alpha-synuclein propagates through neural networks

Masami Masuda-Suzukake[1], Takashi Nonaka[1], Masato Hosokawa[2], Maki Kubo[1], Aki Shimozawa[1], Haruhiko Akiyama[2] and Masato Hasegawa[1*]

Abstract

Background: α-Synuclein is the major component of filamentous inclusions that constitute the defining characteristic of Parkinson's disease, dementia with Lewy bodies and multiple system atrophy, so-called α-synucleinopathies. Recent studies revealed that intracerebral injection of recombinant α-synuclein fibrils into wild-type mouse brains induced prion-like propagation of hyperphosphorylated α-synuclein pathology. However, the propagation mechanisms of α-synuclein have not been fully elucidated.

Results: In this study, in order to establish where and how α-synuclein pathology propagates, we injected recombinant mouse α-synuclein fibrils into three different brain areas (substantia nigra, striatum, and entorhinal cortex) of wild-type mice and compared the resulting distributions of α-synuclein pathology at 1 month after injection. Distinct patterns of pathology were observed in mice injected at the different sites. Within one month after injection, the pathology had spread to neurons in areas far from the injection sites, especially areas with direct neural connections to the injection sites. Surprisingly, phosphorylated tau and TDP-43 pathologies were also observed in mice injected with α-synuclein fibrils into striatum and entorhinal cortex at one month after injection. Phosphorylated tau and TDP-43 were accumulated in dot-like inclusions, but these were rarely colocalized with α-synuclein pathology. It seems that accumulation of α-synuclein has a synergistic effect on tau and TDP-43 aggregation. Additionally, intracerebral injection with sarkosyl-insoluble fraction prepared from wild-type mice injected synthetic α-synuclein fibrils can also induce phosphorylated α-synuclein pathology in wild-type mice.

Conclusions: Our data indicate that α-synuclein aggregation spread by prion-like mechanisms through neural networks in mouse brains.

Keywords: α-Synuclein, Lewy bodies, Propagation, Prion

Introduction

Parkinson's disease (PD) and dementia with Lewy bodies (DLB) are progressive neurodegenerative diseases characterized by appearance of Lewy bodies (LBs) and Lewy neurites (LNs) [1]. α-Synuclein (αsyn) is the major component of LBs and LNs, and is deposited in a hyperphosphorylated form in β-sheet-rich amyloid fibrils [2-5]. Five missense mutations in the αsyn gene and occurrence of gene multiplication have been identified in the familial forms of PD and DLB [6-13]. Moreover, it was reported that the mutations affect amyloid fibril formation *in vitro*, either accelerating fibril formation [14-16] or resulting in formation of fibrils that are more fragile and easy to propagate than wild-type (WT) fibrils [17]. These results clearly indicate that abnormalities of αsyn can induce PD and DLB. Distribution of αsyn pathology in brains with sporadic PD occurs from olfactory bulb and/or brainstem, and spreads to other brain regions concomitantly with progression of disease symptoms [18,19]. Thus, spread of αsyn pathology in the brain can be regarded as the underlying mechanism of progression of these diseases. Recently intracerebral injection of synthetic αsyn fibrils and/or insoluble αsyn from diseased brain was shown to induce αsyn pathology that propagated throughout the brain in a prion-like manner in WT mouse [20,21], αsyn transgenic mouse [22-24] and monkey [25]. However, the mechanisms through which exogenous abnormal fibrils enter

* Correspondence: hasegawa-ms@igakuken.or.jp
[1]Department of Neuropathology and Cell Biology, Tokyo Metropolitan Institute of Medical Science, 2-1-6 Kamikitazawa, Setagaya-ku, Tokyo 156-0057, Japan
Full list of author information is available at the end of the article

neurons and through which insoluble αsyn is transported to other neurons remain unknown.

To investigate where αsyn pathologies develop and how they propagate, we injected recombinant αsyn fibrils into substantia nigra, striatum, or entorhinal cortex of WT mice, and compared the spreading patterns and distribution of phosphorylated αsyn pathologies at 1 month after intracerebral injections. Our results clearly suggest that propagation of pathological αsyn occurred along neural circuits and involved trans-synaptic transport. We also showed that αsyn pathology induced tau and TDP-43 accumulation in WT mice, similar to that seen in DLB brains. This mouse model should be useful for elucidating mechanisms of disease progression of synucleinopathy and also for development of novel disease-modifying drugs.

Materials and methods

Antibodies

Antibodies used in this study are summarized in Additional file 1: Table S1. 1175 polyclonal antibody was raised against an αsyn peptide phosphorylated at serine 129 [21,26]. Anti-phosphorylated αsyn mouse monoclonal antibody, #64 [5] and anti-human αsyn specific mouse monoclonal antibody, LB509 [27] were kindly provided from Dr. Iwatsubo. Rabbit polyclonal pS396 antibody (Calbiochem) is specific for phosphorylated tau at serine 396; biotin-AT8 (Thermo Scientific) is specific for phosphorylated tau at serine 202/threonine 205; anti-mouse αsyn rabbit monoclonal antibody (Cell Signaling Technology) is specific for mouse αsyn. Rabbit polyclonal pTDP-43 antibody is specific for phosphorylated at serine 409/410 [28].

Preparation of recombinant αsyn monomer and fibrils

Mouse αsyn cDNA in bacterial expression plasmid pRK172 was used. αSyn were expressed in *Escherichia coli* BL21 (DE3) cells and purified using boiling, Q-sepharose ion exchange chromatography and ammonium sulfate precipitation. Purified αsyn protein was dialyzed against 30 mM Tris–HCl, pH 7.5, and cleared using ultracentrifugation at 113,000 g for 20 min. Protein concentration was determined by reverse phase HPLC. Proteins were loaded on an Aquapore RP-300 column (PerkinElmer Brownlee) equilibrated in 0.09% trifluoroacetic acid with linear gradient of acetonitrile 0 to 50% at a flow rate of 1 ml/min [21]. Purified mouse αsyn monomer (7 mg/ml) in 30 mM Tris–HCl, pH 7.5, containing 0.1% NaN_3 was incubated at 37°C in a shaking incubator at 200 rpm for 72 h. αSyn fibrils were pelleted by spinning at 113,000 g for 20 min and

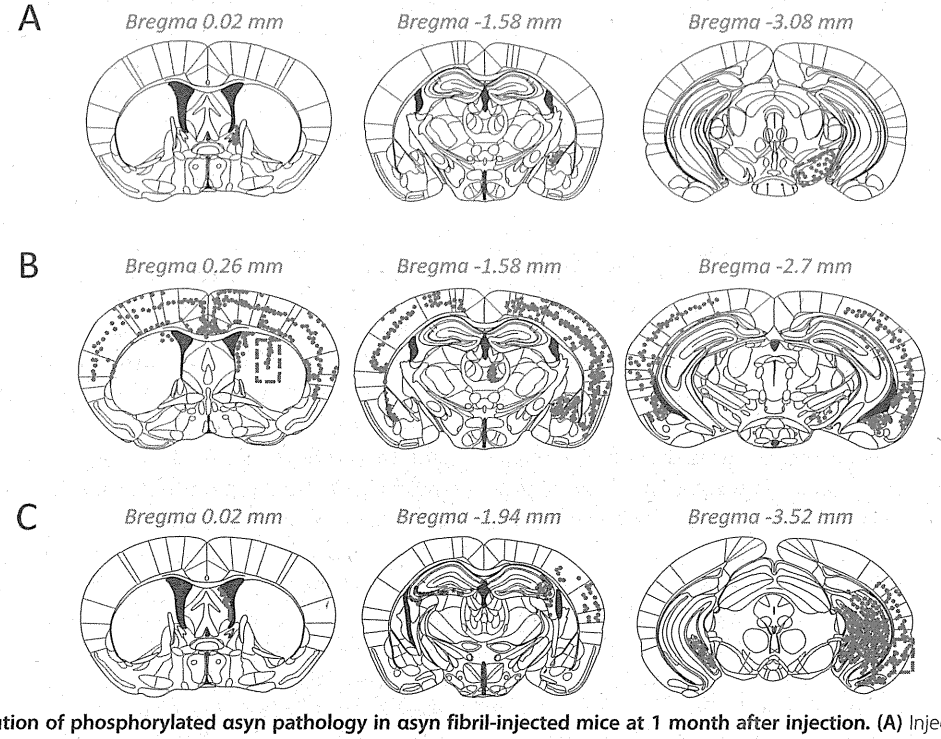

Figure 1 Distribution of phosphorylated αsyn pathology in αsyn fibril-injected mice at 1 month after injection. **(A)** Injection into SN induced αsyn pathology mainly in SN (3.08 mm posterior to bregma), amygdala (1.58 mm posterior to bregma) and stria terminalis (0.02 mm anterior to bregma). **(B)** Injection into Str induced severe αsyn pathology throughout the brain, including Str (0.26 mm anterior to bregma), amygdala (1.58 mm posterior to bregma), SN (2.70 mm posterior to bregma) and a wide range of cortex. **(C)** Injection into EC induced αsyn pathology that was concentrated in EC (3.52 mm posterior to bregma), dentate gyrus (3.52 mm posterior to bregma), CA3 (3.52 mm posterior to bregma), fimbria (1.94 mm posterior to bregma), and septal nucleus (0.02 mm anterior to bregma). Blue-dashed box and red dots indicate the injection site and psyn pathology, respectively.

suspended in PBS. αSyn fibrils were sonicated with a ultrasonic homogenizer (VP-5S, TAITEC) before use. To determine the concentration, fibrils were dissolved in 8 M guanidine hydrochloride and analyzed by RP-HPLC as described above.

Mice

C57BL/6 J mice, used as WT mice, were purchased from CLEA Japan, Inc. αSyn (SNCA) knockout mice [29] were purchased from the Jackson Laboratory.

Stereotaxic surgery

Four- to six-month-old mice anesthetized with 50 mg/kg pentobarbital sodium were unilaterally injected with 10 μg of recombinant mouse αsyn fibrils into substantia nigra (SN, n = 6) (A-P: −3.0 mm; M-L: −1.3 mm; D-V: −4.7 mm from the bregma and dura) [21], striatum (Str, n = 6) (A-P: 0.2 mm; M-L: −2.0 mm; D-V: −2.6 mm) [20], or entorhinal cortex (EC, n = 6) (A-P: −3.1 mm; M-L: −4.0 mm; D-V: −2.7 mm). Mice were anesthetized with isoflurane and killed by decapitation. For immunohistochemistry (IHC, n = 3), brains were fixed in 10% formalin neutral buffer solution (Wako). For biochemical analysis (n = 3), brains were snap-frozen on dry ice and stored at −80°C. All experimental protocols were approved by the Animal Care and Use Committee of the Tokyo Metropolitan Institute of Medical Science.

Peripheral injection of αsyn

For intraperitoneal injection, 2-month-old C57BL/6 J mice were injected intraperitoneally with 100 μg of mouse αsyn monomer or fibrils. At 6 months after injection, the pathology of mouse brains in both groups (n = 3 each) was tested by immunohistochemistry (IHC). For oral administration, 2- or 3-month-old C57BL/6 J mice were orally administrated with 400 μg of human αsyn monomer, human αsyn fibrils, mouse αsyn monomer or mouse αsyn fibrils every two weeks for 4 times. At 12 months post final administration, pathology in mouse brains (n = 3 each) was analyzed by IHC.

Immunohistochemistry

Fixed brains were cut on a vibratome (Leica) at 50 μm thickness. For high-sensitivity detection, mouse brain sections were treated with formic acid for 30 min, washed, and boiled at 100°C for 30 min. The sections were then incubated with 0.5% H_2O_2 in methanol to inactivate endogenous peroxidases, blocked with 10% calf serum in PBS, and immunostained with appropriate antibodies. After incubation with the biotinylated-secondary antibody (Vector), labeling was detected using the ABC staining kit (Vector).

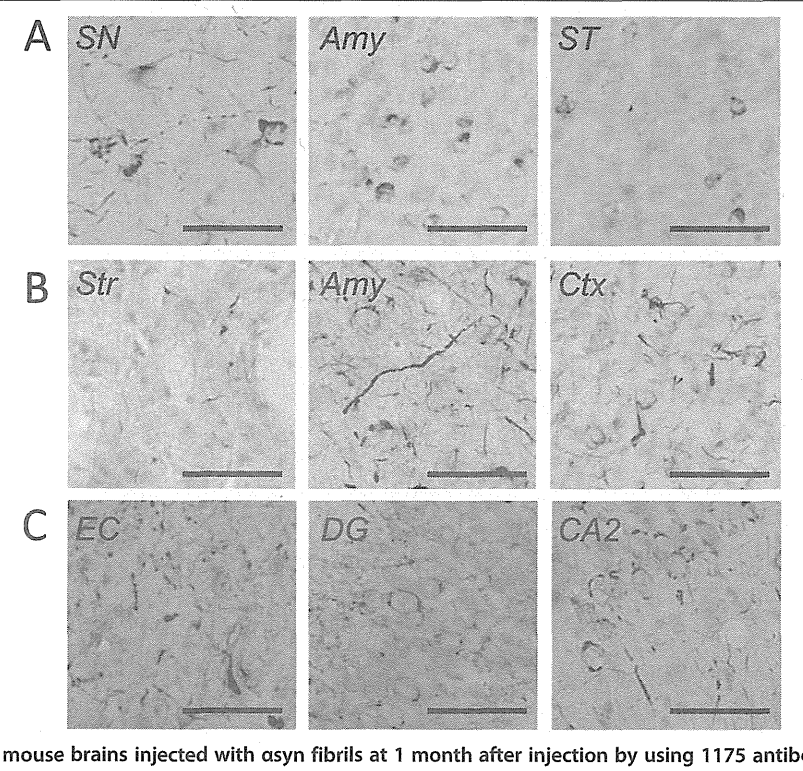

Figure 2 Staining of WT mouse brains injected with αsyn fibrils at 1 month after injection by using 1175 antibody. (A) Psyn pathology in mice injected into SN. **(B)** Psyn pathology in mice injected into Str. **(C)** Psyn pathology in mice injected into EC. SN: substantia nigra, Amy: amygdala, ST: stria terminalis, Str: striatum, Ctx: cortex, EC: entorhinal cortex, DG: dentate gyrus. Scale bar represents 50 μm.

Confocal microscopy

For double-label immunofluorescence to detect phosphorylated αsyn and tau, brain sections were incubated overnight at 4°C in a cocktail of #64 antibody and anti-pS396 antibody. The sections were washed and incubated in a cocktail of Alexa568-conjugated goat anti mouse IgG (Molecular Probes) and Alexa488-conjugated goat anti rabbit IgG (Molecular Probes). After further washing, sections were stained with TOPRO-3, coverslipped with Vectashield (Vector) and observed with a laser-scanning confocal fluorescence microscope (LSM5 PASCAL; Carl Zeiss).

Biochemical analysis

Biochemical analysis of mouse brains (n = 3 per group) was conducted as described previously [21]. Briefly, brains were homogenized in 20 volumes (w/v) of buffer A (10 mM Tris–HCl, pH 7.4, 0.8 M NaCl, 1 mM EGTA and 10% sucrose), then spun at 100,000 g for 30 min at 4°C, and the supernatant was retained as buffer-soluble

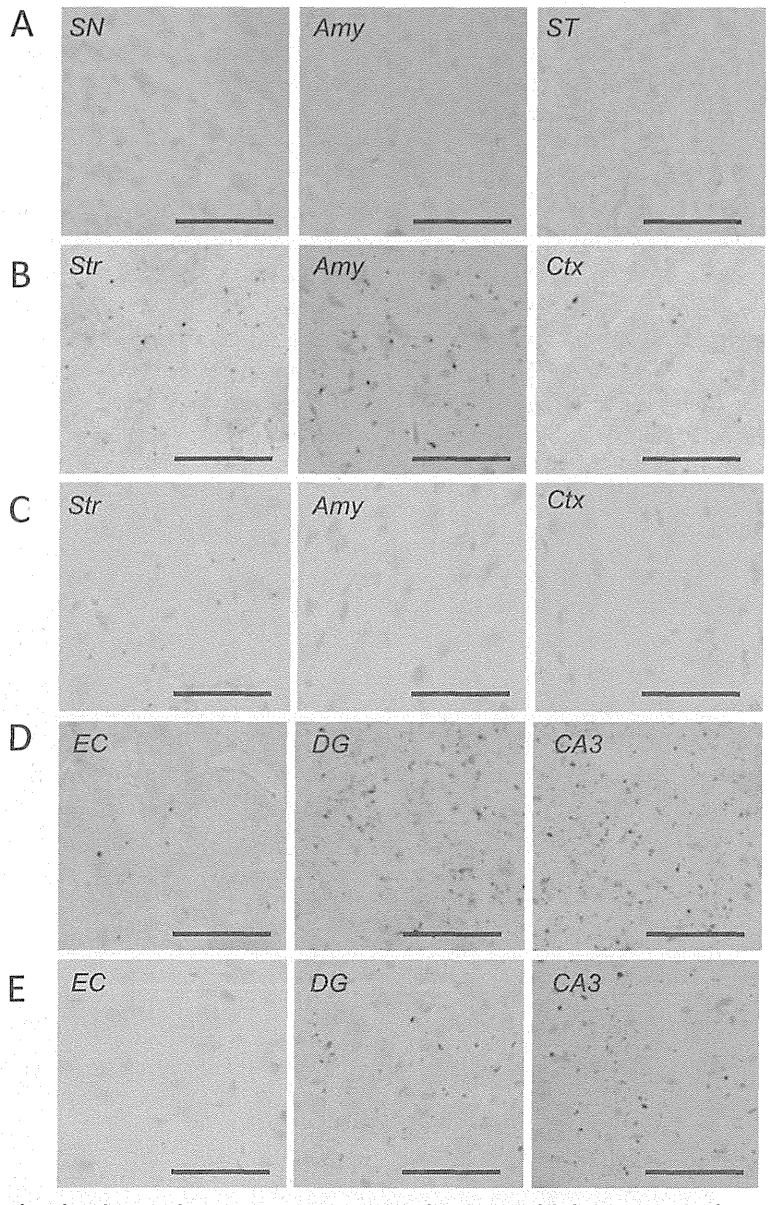

Figure 3 Induction of phosphorylated tau inclusions in WT mice injected with αsyn fibrils at 1 month after injection. (A) Phosphorylated tau was not accumulated in mice injected into SN, based on staining with anti-pS396 antibody. **(B-C)** Dot-like tau inclusions were observed in mice injected into Str by using anti-pS396 antibody **(B)** and AT8 **(C) (D-E)**. Dot-like tau inclusions were also detected in mice injected into EC by using anti-pS396 antibody **(D)** and AT8 **(E)**. SN: substantia nigra, Amy: amygdala, ST: stria terminalis, Str: striatum, Ctx: cortex, EC: entorhinal cortex, DG: dentate gyrus. Scale bar represents 50 μm.

fraction. The pellet was homogenized in 20 volumes of buffer A containing 1% Triton X-100 and incubated for 30 min at 37°C. After centrifugation at 100,000 g, the Triton-insoluble pellet was further homogenized in buffer A containing 1% sarkosyl and incubated at 37°C for 30 min. Samples were spun at 100,000 g for 30 min. The sarkosyl-pellet was sonicated in 30 mM Tris–HCl, pH 7.4, and used for immunoblotting as sarkosyl-insoluble fraction. The samples were subjected to SDS-PAGE and proteins were electrotransferred onto a polyvinylidene difluoride membrane, probed with appropriate antibodies and detected as described previously [21].

Behavioral tests

For behavioral tests, C57BL/6 J male mice were used. Mouse αsyn fibrils (10 μg) were injected into SN (n = 10), Str (n = 15), or EC (n = 14) of 3-month-old mice, and the same amount of mouse αsyn monomer was injected into SN (n = 9), Str (n = 8), or EC (n = 8) of control mice. At 3 months after injection, motor and cognitive activities were evaluated as described below.

Rotarod test

Motor coordination and balance were measured in terms of performance on the rotarod. Mice were placed on 3-cm diameter rods and the speed of the rotation was increased from 0 to 40 rpm over 5 min. Latency to fall was recorded. Each mouse was tested three times and the average was used. Statistical analyses were performed using Student's *t*-test.

Wire hang test

Neuromuscular abnormalities were tested with the wire hang test. The mouse was placed on a wire cage lid, which was waved gently so that the mouse gripped the wire and then inverted. Latency to fall was recorded with a 300-sec cut-off time. The test was conducted three times and statistical analyses were performed using Student's *t*-test.

Y-maze test

The Y-maze apparatus (Muromachi kikai) consisted of three arms (40 cm × 3 cm) made of grey plastic joined in the middle to form a Y shape. Mice were placed into one of the arms of the maze and allowed to freely explore the three arms for an 8-min session. Alternation between arms was recorded. The Y-maze test was conducted twice. Statistical analyses were performed using Student's *t*-test.

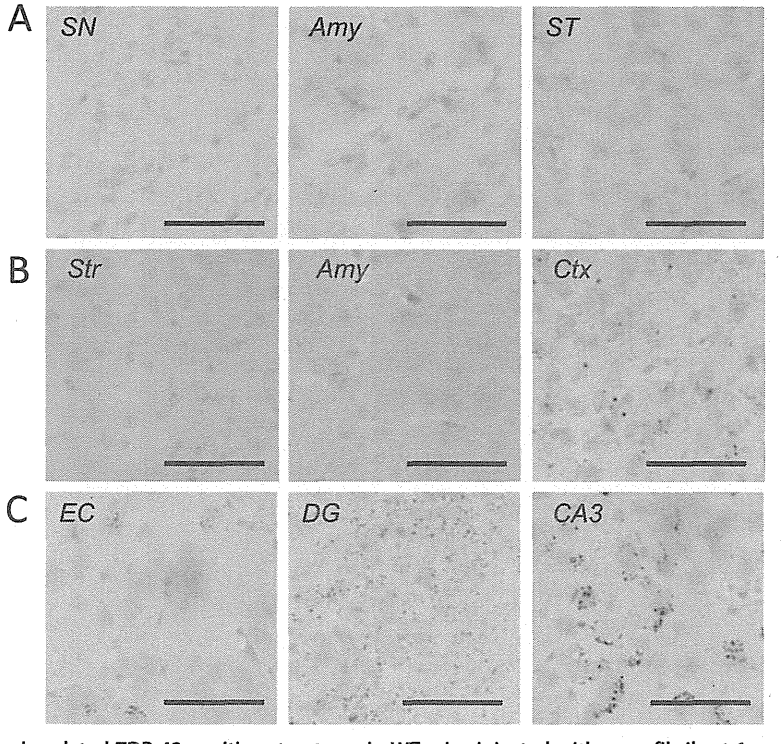

Figure 4 Induction of phosphorylated TDP-43-positive structures in WT mice injected with αsyn fibrils at 1 month after injection. **(A)** Phosphorylated TDP-43 was not accumulated in mice injected into SN, based on staining with anti-pS409/410 antibody. **(B)** Dot-like TDP-43 inclusions were observed in mice injected into Str. **(C)** Dot-like TDP-43 inclusions were also detected in mice injected into EC. SN: substantia nigra, Amy: amygdala, ST: stria terminalis, Str: striatum, Ctx: cortex, EC: entorhinal cortex, DG: dentate gyrus. Scale bar represents 50 μm.

Transmission experiments

Recombinant human αsyn fibrils (10 μg) were injected into SN of 4-month-old WT mice (n = 4). At 9 months after injection, sarkosyl-insoluble pellets were prepared from the whole brains as described above, collected in one tube, and stored at −80°C until use. Sarkosyl-insoluble pellets were suspended in 100 μl PBS and sonicated for 30 seconds (TAITEC, VP-5S), and 5-μl aliquots were injected into Str of 4-month-old WT mice (n = 10). At 3 months post injection, pathology was analyzed by IHC.

Results

We investigated the spread of αsyn pathology in brains of mice after unilateral injection of recombinant mouse αsyn fibrils into SN, Str, or EC. We confirmed the purity of recombinant αsyn monomer and fibrils used in this study; they didn't contain any contaminants (Additional file 1: Figure S1). Using highly sensitive immunohistochemistry (IHC) with anti-phosphorylated αsyn (psyn) antibody 1175, we evaluated αsyn pathology in the brains at 1 month after injection. The distribution of αsyn pathology observed in these mice is illustrated in Figure 1. In mice injected into SN (Figure 1A), abnormal psyn pathology was restricted mainly to SN (3.08 mm posterior to bregma), amygdala (1.58 mm posterior to bregma), and stria terminalis (0.02 mm anterior to bregma) of the hemisphere on the injection side. In these mice, psyn was accumulated in neurites and soma (Figure 2A). In mice injected into Str, psyn pathology was widely distributed bilaterally throughout the brain, including Str (0.26 mm anterior to bregma), amygdala (1.58 mm posterior to bregma), SN (2.70 mm posterior to bregma) and cortex (Figure 1B). Psyn pathology was accumulated mainly in neurites, and partly in soma (Figure 2B). Injection of αsyn fibrils into EC induced severe psyn pathology in EC (3.52 mm posterior to bregma), dentate gyrus (3.52 mm posterior to bregma), hippocampal CA3 region (1.94 and 3.52 mm posterior to bregma), fimbria (1.94 mm posterior to bregma), and septal nuclei (0.02 mm anterior to bregma) on the injection side, as well as moderate psyn pathology in hippocampus on the contralateral side (Figure 1C). Psyn pathology was mainly observed in neurites and perinuclear regions (Figure 2C). No such psyn accumulation was detected in αsyn KO mice injected with αsyn fibrils into Str (Additional file 1: Figure S2A). Thus, there are major differences among these mice in the development and spread of αsyn pathologies, demonstrating that the propagation pattern depends upon the injection site.

To investigate whether other pathologies are also induced by the injection of αsyn fibrils, we performed IHC analysis using anti-tau, anti-TDP and anti-Aβ antibodies. No tau pathology was observed in mice injected into SN

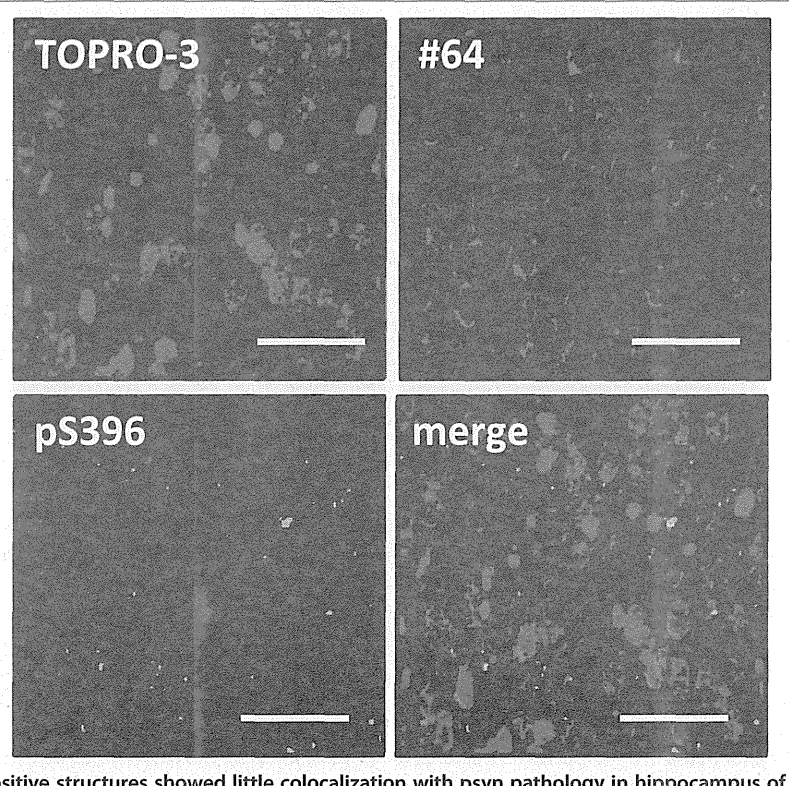

Figure 5 Dot-like ptau-positive structures showed little colocalization with psyn pathology in hippocampus of mice injected with αsyn fibrils into EC at 1 month after injection. Brain sections were double-labeled with anti-psyn antibody (#64, red) and anti-ptau antibody (pS396, green). Scale bar represents 50 μm.

(Figure 3A). However, surprisingly, in mice injected into Str, pS396-positive dot-like structures were observed in Str, amygdala, and cortex (Figure 3B). Anti-phosphorylated tau (ptau) antibody AT8 also stained these structures in Str (Figure 3C). Similar ptau-positive dot-like structures were also observed with anti-pS396 antibody in EC, dentate gyrus and CA3 of the mice injected into EC, and were most frequent in CA3 (Figure 3D). Similar staining was observed in CA3 and dentate gyrus with AT8 antibody (Figure 3E). Furthermore, phosphorylated TDP-43 was also accumulated in mice injected into Str and EC (Figure 4B,C), although it was not detected in mice injected into SN (Figure 4A) at 1 month after injection. Aβ pathology was never observed in αsyn fibril-injected mice, regardless of injection site (Additional file 1: Figure S3). The tau and TDP-43 pathologies differed from psyn pathology in both shape and localization; most psyn pathologies were not colocalized with ptau-positive structures and the overlap was small (Figure 5).

To confirm the accumulation of these proteins and to analyze them biochemically, we next investigated sarkosyl-insoluble fractions of these mice brains at 3 months after injection into SN, Str or EC (Figure 6). Sarkosyl-insoluble psyn was detected in both the right and left hemispheres of all these mice, though it was more abundant on the injection side. The accumulation was most abundant on the injection side (right brain) in mice injected into Str, and less abundant on the uninjected side in mice injected into SN or EC. The banding patterns of sarkosyl-insoluble psyn were identical among these mice, regardless of the injection site, and were indistinguishable from that of DLB brain (Figure 6 upper). Anti-mouse αsyn antibody showed the same banding pattern as psyn antibody (Figure 6 middle). The 15, 22, 30 and 35 kDa bands correspond to monomer, monoubiquitinated αsyn, dimer and ubiquitinated dimer, respectively. Moreover, sarkosyl-insoluble ptau was detected in the right hemisphere of mice injected into Str, where the most abundant tau inclusions were observed (Figure 6 lower). On the other hand, αsyn and tau accumulations were not observed in αsyn KO mice injected with fibrils into Str (Additional file 1: Figure S4). These results indicate that inoculation of αsyn fibrils converted mouse αsyn at the injection sites to an abnormal form, that this change propagated from the injection site to the contralateral side of the brain, and that inoculation into Str also induced tau pathology.

Next, we analyzed motor and cognitive functions of these mice at 3 months after injection (Figure 7). Mice injected with αsyn fibrils into SN and Str showed poorer performance on the rotarod test compared with control mice injected with soluble αsyn (Figure 7A). Mice injected into SN also performed poorly on the wire hang test (Figure 7B). Cognitive dysfunction was not observed in any group in the Y-maze test (Figure 7C).

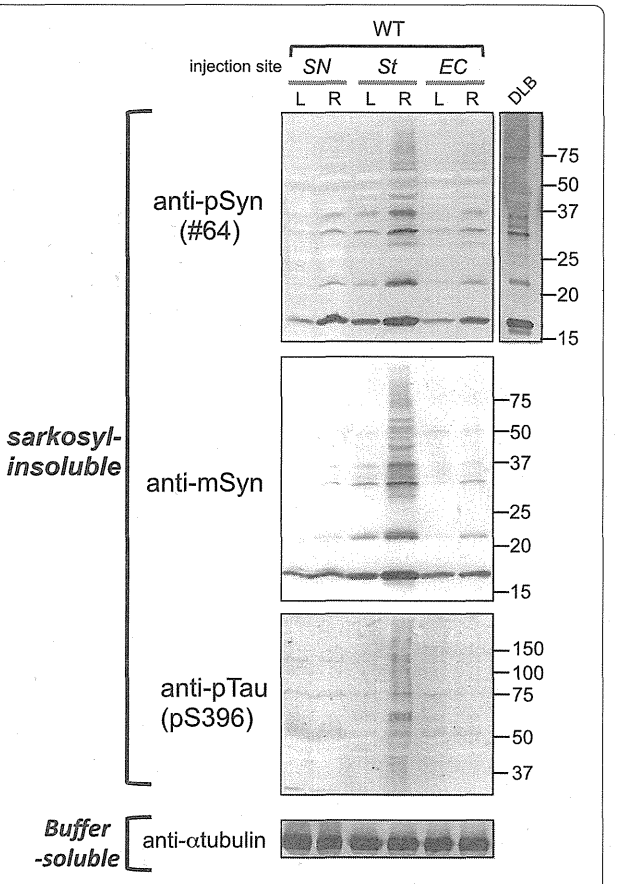

Figure 6 Intracerebral injections with αsyn fibrils induced accumulation of endogenous αsyn and tau in WT mice. At 3 months after injection, sarkosyl-insoluble fractions were prepared from the right and left brains and analyzed by immunoblotting with #64, anti-mouse syn and anti-pS396 antibodies. Band patterns of insoluble psyn were identical to that of DLB brain. Insoluble ptau was also accumulated in mouse brains showing abundant accumulation of αsyn. L: left brain, R: right brain.

Finally, to examine whether insoluble αsyn induced in WT mice shows prion-like propagation behavior, we assessed the transmissibility of insoluble αsyn prepared from fibril-injected WT mouse brains. In brief, sarkosyl-insoluble αsyn was prepared from WT mouse brains injected with recombinant αsyn fibrils and was injected into Str of other WT mouse brains (Figure 8A, B). Induction and propagation of psyn pathology were examined by IHC. At 3 months after injection, psyn pathology was observed in Str (0.26 mm anterior to bregma) and had also propagated to amygdala (1.46 mm posterior to bregma) and SN (3.08 mm posterior to bregma) (Figure 8C). The distribution of psyn pathology is illustrated in Figure 8D. These data clearly showed that insoluble αsyn derived from WT mice injected with αsyn fibrils exhibits prion-like transmissibility.

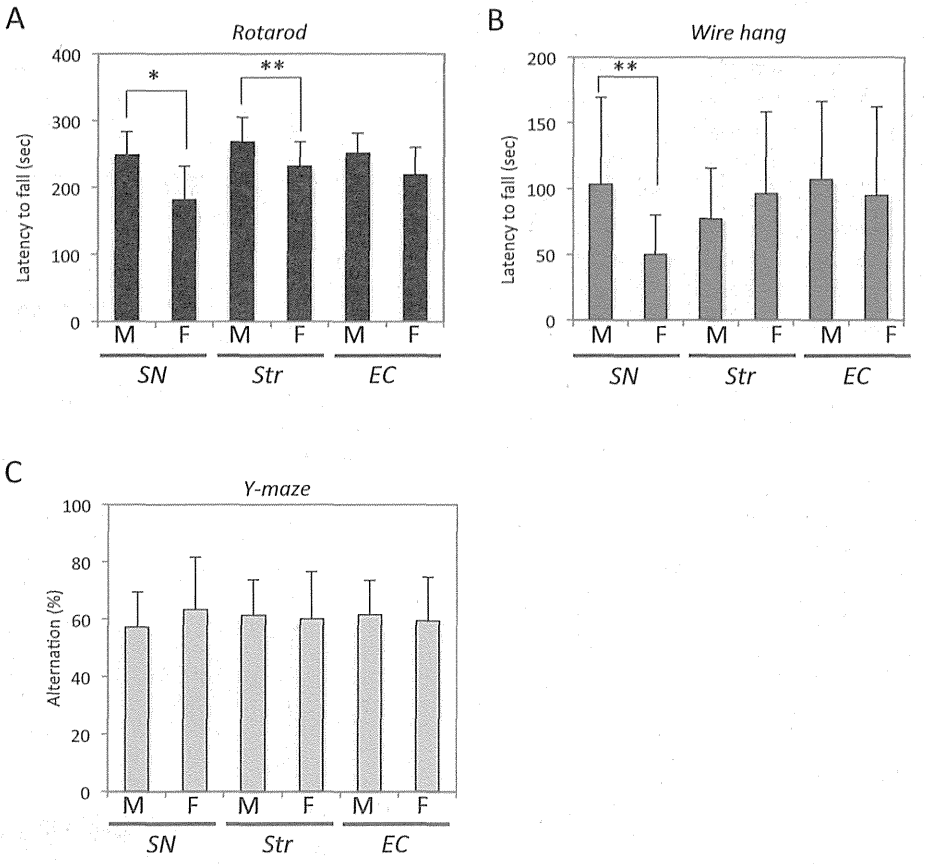

Figure 7 Fibril-injected mice showed motor dysfunctions compared to monomer-injected mice at 3 months after injection. (A) Rotarod test. Mice injected into SN and Str showed lower performance in the rotarod test. **(B)** Wire hang test. **(C)** Y-maze test. All error bars indicates mean ± S. E. M. *$p < 0.01$, **$p < 0.05$. M: αsyn monomer-injected, F: αsyn fibril-injected.

Discussion

Luk et al. and we have established that insoluble αsyn shows prion-like propagation behavior in WT mouse brain [20,21], but the mechanism of spreading remains poorly understood. In this study, we investigated the spread and distribution pattern of psyn pathology in mouse brain injected with recombinant αsyn fibrils into three different brain regions: SN, Str, and EC. We assessed the distribution at 1 month post injection by using highly sensitive IHC. Pretreatment of brain sections with formic acid and heat enabled detection of psyn pathology at only 1 month after injection. When αsyn fibrils were injected into SN, psyn pathology only appeared in the central nucleus of amygdala and stria terminalis, which are located far from SN, while there was no detectable psyn pathology around SN (Figure 1A). Amygdala is connected with SN [30], and stria terminalis serves as a major output pathway of the central nucleus of amygdala. These findings strongly indicate that spreading of psyn pathology does not occur by simple diffusion or nonspecific transport. In the case of injection into Str, psyn pathology was observed in amygdala, SN and a wide range of cortices (Figure 1B). Str has direct projection to SN and amygdala [31], and many parts of the neocortex innervate the Str [32]. Injection into EC induced pathology in EC, dentate gyrus, hippocampal CA3, fimbria and septal nucleus (Figure 1C). Dentate gyrus receives projection from EC via the perforant pathway, and septal nucleus and fimbria have direct connections with hippocampus. Therefore, the data strongly suggest that propagation of pathological αsyn occurs via axonal transport and a trans-synaptic pathway, in accordance with reports that αsyn fibrils can be internalized by neurons and transferred from axons to second-order neurons in culture [33] and in animal models [34,35]. In patients with sporadic PD, the distribution of Lewy bodies and Lewy neurites seems to spread retrogradely [18,36]. In the present study, focusing on Str and SN, injection with αsyn fibrils into Str induced αsyn pathology in SN at 1 month after injection (Figure 1B). However, injection into SN did not induce pathology in Str at that time (Figure 1A), and pathology only became apparent in Str at 3 months after injection [21], indicating there is a dominant direction of spread. Propagation from EC to

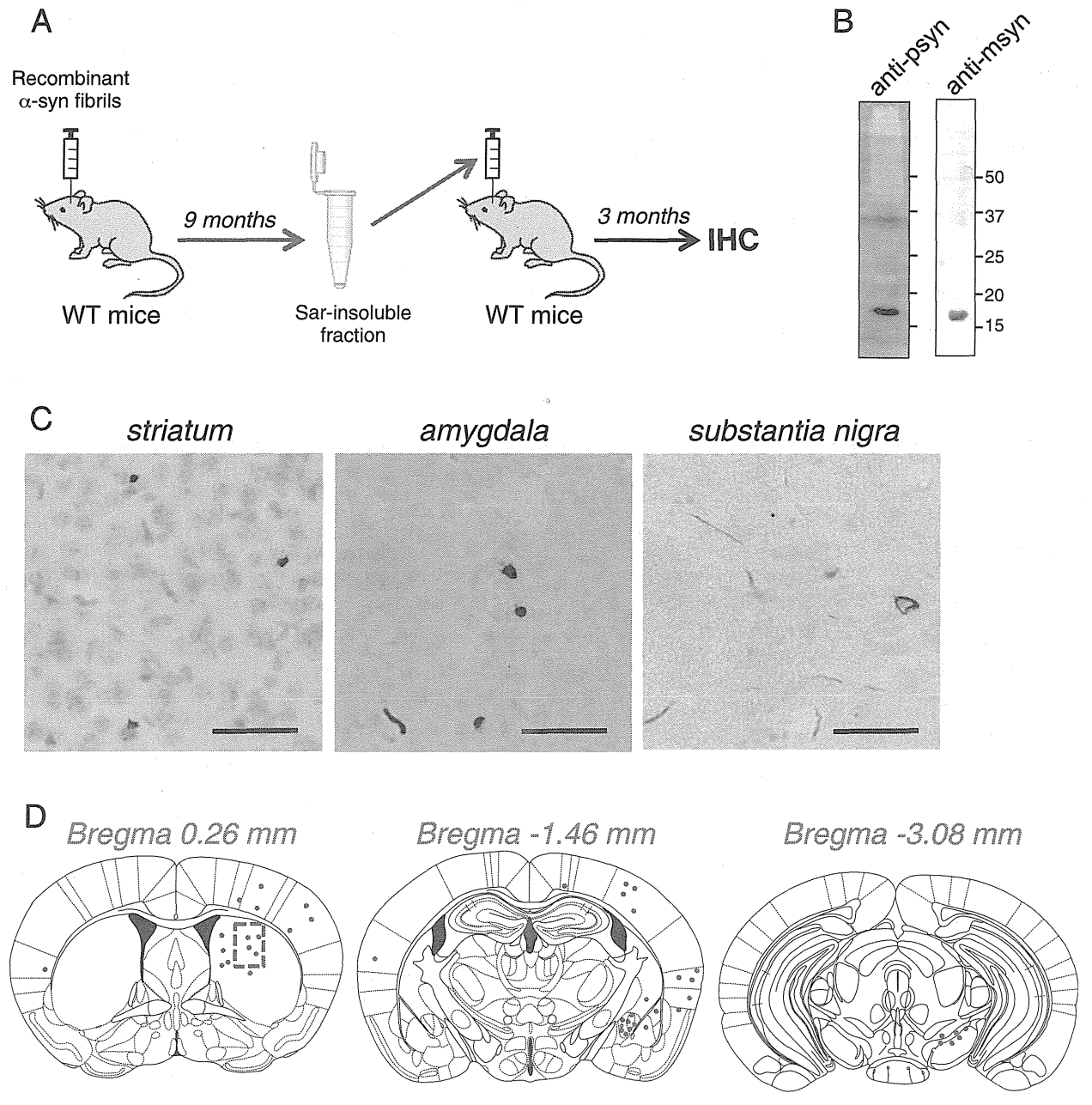

Figure 8 Sequential transmission of insoluble αsyn. (A) Schematic diagrams of transmission experiments. Sarkosyl-insoluble fractions were prepared from WT mouse brains injected with recombinant αsyn fibrils at 9 months post-injection and intracerebrally injected into 4-month-old WT mice. At 3 months after injection, transmission of αsyn pathology was analyzed by IHC. **(B)** Immunoblot of sarkosyl-insoluble fractions from WT mice at 9 months post-injection with #64 antibody and anti-msyn antibody. **(C)** Psyn pathology was observed mainly in Str, amygdala and SN with 1175 antibody. Scale bar represents 50 μm. **(D)** Distribution of psyn pathology in WT mouse brains injected with sarkosyl-insoluble fractions. Blue-dashed box and red dots indicate the injection site (Str) and psyn pathology, respectively.

dentate gyrus via the perforant pathway might occur via anterograde transport (Figure 1C). At least under our experimental conditions, propagation of αsyn seems to occur via both anterograde and retrograde transport processes. Thus, the predominant direction of spread presumably depends on cell types or brain areas. Similarly, tau is also reported to propagate via a trans-synaptic pathway in animal models [37,38]. Thus, axonal transport and trans-synaptic transport appear to be common pathways of propagation of intracellular aggregated proteins.

In addition, we found that tau and TDP-43 accumulation also occurred in WT mice injected with αsyn fibrils

into Str and EC at 1 month after injection (Figures 3B-E and 4). The morphological patterns of tau and TDP-43 accumulation were apparently different from that of αsyn pathology (Figures 2, 3 and 4) and there was little colocalization (Figure 5), as in DLB brains [39,40] and a DLB mouse model [41]. Recently, Guo et al. reported that there are two strains of recombinant αsyn fibrils, strains A and B, and the two strains differently affect tau inclusion formation [42]. They reported that strain A (preformed fibrils) only infrequently induced tau inclusions and psyn pathology showed little colocalization with tau inclusions, whereas strain B (generated through repetitively seeded fibrillization *in vitro*) efficiently induced tau inclusions that were highly colocalized in neurons. The αsyn fibrils we used in this study are similar to strain A, and in agreement with their work [42], we also detected small amounts of tau inclusions that showed little colocalization with αsyn pathology. In addition, tau accumulation was not observed in αsyn KO mice injected with αsyn fibrils by biochemical analysis (Additional file 1: Figure S4) or IHC (Additional file 1: Figure S2B). Thus, tau accumulation was induced by αsyn accumulation, and this occurred through a synergistic effect rather than a cross-seeding effect. The tau accumulation might be caused by a secondary effect of αsyn accumulation, such as dysfunction of cellular activity [43,44] or abnormality in protein degradation machinery [45].

Biochemical analysis clearly showed that accumulated αsyn was phosphorylated and ubiquitinated similarly to that in DLB brain, regardless of injection site (Figure 6). This indicates that injection with the same fibrils as seeds induces αsyn aggregation in the same fashion, as is the case with prion strains.

Furthermore, αsyn fibril-injected mice showed modest motor abnormalities compared to the monomer-injected mice at 3 months after injection (Figure 7). This strongly suggests that propagation of psyn pathology induced motor phenotypes, although we could not detect cognitive dysfunction in the Y-maze test. It is possible that this is because we injected αsyn fibrils unilaterally, and the functions of the contralateral side of brain might be well maintained. In our previous study, we could not detect any abnormalities in fibril-injected mice at 6 months after injection [21]. The discrepancy may have arisen from differences in the test conditions, because in the previous study, we used female mice injected with human αsyn fibrils, whereas in this study we used male mice injected with mouse αsyn. Mouse αsyn fibrils propagate more efficiently in WT mice than do human fibrils [21], and we think this was the main reason why we could detect motor abnormalities in the present study.

We next examined if insoluble αsyn accumulated in WT mice shows transmissibility. Our results demonstrate that insoluble αsyn accumulated in WT mice can induce αsyn pathology in other WT mice (Figure 8C, D), analogously to prion transmission. We also examined intraperitoneal injection or oral administration with αsyn fibrils into WT mice (see Materials and methods), but failed to detect any psyn pathology in the central nervous system at 6 months or 14 months after injection, respectively (data not shown).

Conclusions

Intracerebral injection with αsyn fibrils into WT mouse brains enables to induce phosphorylated αsyn pathology and the distribution of pathology depends on the injection sites. Furthermore, αsyn pathology has a synergistic effect on tau and TDP-43 aggregation. We conclude that αsyn fibrils have prion-like transmissibility and it might spread via axonal and trans-synaptic transports in mouse brains.

Additional file

Additional file 1: Table S1. Antibodies used in this study. **Figure S1.** HPLC charts of recombinant mouse αsyn used in this study. Mouse syn monomer showed only one peak that is derived from msyn monomer. Mouse syn fibril gave two peaks at 0.14 min (guanidine HCl) and at 6.8 min (msyn fibril). **Figure S2.** αSyn and tau accumulation was never observed in fibril-injected αsyn KO mice at 3 months after injection. **(A)** No psyn-positive pathology was observed with 1175 antibody. **(B)** Tau accumulation was not detected with pS396 antibody. Str: striatum, Amy: amygdala, SN: substantia nigra, sensory ctx: sensory cortex. Scale represents 50 μm. **Figure S3.** Aβ accumulation was not observed in αsyn fibril-injected WT mice at 1 month post injection. Sections were stained with anti-mouse Aβ antibody. Mice injected into SN **(A)**, Str **(B)**, and EC **(C)**. SN: substantia nigra, Amy: amygdala, ST: stria terminalis, Str: striatum, Ctx: cortex, EC: entorhinal cortex, DG: dentate gyrus. Scale represents 50 μm. **Figure S4.** Biochemical analysis of αsyn KO mice injected with human αsyn fibrils. The brain was divided into two parts at the longitudinal fissure of the cerebrum. Sarkosyl-insoluble fractions were obtained from the right and left brains, and analyzed by immunoblotting with #64, LB509 or anti-mouse αsyn antibodies. Exogenous human αsyn fibrils were detected in sarkosyl-insoluble fractions and were not phosphorylated at 0 and 7 days after injection. They were subsequently degraded and disappeared within 30 days post injection. Phosphorylated αsyn accumulation was never observed at 90 days after injection.

Competing interests

The authors declare that they have no competing interests.

Authors' contributions

MMS performed stereotaxic surgery, biochemical and IHC studies and wrote the manuscript. MK and AS performed IHC analysis and behavioral tests. TN and MH helped for interpretation of data. HA provided antibodies and helpful advice. MH performed study design and wrote the manuscript. All authors read and approved the final manuscript.

Acknowledgements

This work was supported by MEXT KAKENHI Grant Numbers 12937622, 12901980 (to M.H.), JSPS KAKENHI Grant Number 23700433 (to M.M-S.) and MHLW Grant Number 12946221 (to M.H.).

Author details

[1]Department of Neuropathology and Cell Biology, Tokyo Metropolitan Institute of Medical Science, 2-1-6 Kamikitazawa, Setagaya-ku, Tokyo 156-0057, Japan. [2]Dementia Research Project, Tokyo Metropolitan Institute of Medical Science, Setagaya-ku, Tokyo, Japan.

Received: 14 July 2014 Accepted: 18 July 2014
Published: 6 August 2014

References

1. Goedert M (2001) Alpha-synuclein and neurodegenerative diseases. Nat Rev Neurosci 2(7):492–501, doi:10.1038/35081564
2. Spillantini MG, Schmidt ML, Lee VM, Trojanowski JQ, Jakes R, Goedert M (1997) Alpha-synuclein in Lewy bodies. Nature 388(6645):839–840, doi:10.1038/42166
3. Spillantini MG, Crowther RA, Jakes R, Hasegawa M, Goedert M (1998) Alpha-Synuclein in filamentous inclusions of Lewy bodies from Parkinson's disease and dementia with lewy bodies. Proc Natl Acad Sci U S A 95(11):6469–6473
4. Baba M, Nakajo S, Tu PH, Tomita T, Nakaya K, Lee VM, Trojanowski JQ, Iwatsubo T (1998) Aggregation of alpha-synuclein in Lewy bodies of sporadic Parkinson's disease and dementia with Lewy bodies. Am J Pathol 152(4):879–884
5. Fujiwara H, Hasegawa M, Dohmae N, Kawashima A, Masliah E, Goldberg MS, Shen J, Takio K, Iwatsubo T (2002) Alpha-Synuclein is phosphorylated in synucleinopathy lesions. Nat Cell Biol 4(2):160–164, doi:10.1038/ncb748
6. Polymeropoulos MH, Lavedan C, Leroy E, Ide SE, Dehejia A, Dutra A, Pike B, Root H, Rubenstein J, Boyer R, Stenroos ES, Chandrasekharappa S, Athanassiadou A, Papapetropoulos T, Johnson WG, Lazzarini AM, Duvoisin RC, Di Iorio G, Golbe LI, Nussbaum RL (1997) Mutation in the alpha-synuclein gene identified in families with Parkinson's disease. Science 276(5321):2045–2047
7. Kruger R, Kuhn W, Muller T, Woitalla D, Graeber M, Kosel S, Przuntek H, Epplen JT, Schols L, Riess O (1998) Ala30Pro mutation in the gene encoding alpha-synuclein in Parkinson's disease. Nat Genet 18(2):106–108, doi:10.1038/ng0298-106
8. Zarranz JJ, Alegre J, Gomez-Esteban JC, Lezcano E, Ros R, Ampuero I, Vidal L, Hoenicka J, Rodriguez O, Atares B, Llorens V, Gomez Tortosa E, Del Ser T, Munoz DG, de Yebenes JG (2004) The new mutation, E46K, of alpha-synuclein causes Parkinson and Lewy body dementia. Ann Neurol 55(2):164–173, doi:10.1002/ana.10795
9. Appel-Cresswell S, Vilarino-Guell C, Encarnacion M, Sherman H, Yu I, Shah B, Weir D, Thompson C, Szu-Tu C, Trinh J, Aasly JO, Rajput A, Rajput AH, Jon Stoessl A, Farrer MJ (2013) Alpha-synuclein p.H50Q, a novel pathogenic mutation for Parkinson's disease. Mov Disord 28(6):811–813, doi:10.1002/mds.25421
10. Lesage S, Anheim M, Letournel F, Bousset L, Honore A, Rozas N, Pieri L, Madiona K, Durr A, Melki R, Verny C, Brice A (2013) G51D alpha-synuclein mutation causes a novel parkinsonian-pyramidal syndrome. Ann Neurol 73(4):459–471, doi:10.1002/ana.23894
11. Singleton AB, Farrer M, Johnson J, Singleton A, Hague S, Kachergus J, Hulihan M, Peuralinna T, Dutra A, Nussbaum R, Lincoln S, Crawley A, Hanson M, Maraganore D, Adler C, Cookson MR, Muenter M, Baptista M, Miller D, Blancato J, Hardy J, Gwinn-Hardy K (2003) Alpha-Synuclein locus triplication causes Parkinson's disease. Science 302(5646):841, doi:10.1126/science.1090278
12. Chartier-Harlin MC, Kachergus J, Roumier C, Mouroux V, Douay X, Lincoln S, Levecque C, Larvor L, Andrieux J, Hulihan M, Waucquier N, Defebvre L, Amouyel P, Farrer M, Destee A (2004) Alpha-synuclein locus duplication as a cause of familial Parkinson's disease. Lancet 364(9440):1167–1169, doi:10.1016/S0140-6736(04)17103-1
13. Ibanez P, Bonnet AM, Debarges B, Lohmann E, Tison F, Pollak P, Agid Y, Durr A, Brice A (2004) Causal relation between alpha-synuclein gene duplication and familial Parkinson's disease. Lancet 364(9440):1169–1171, doi:10.1016/S0140-6736(04)17104-3
14. Conway KA, Harper JD, Lansbury PT (1998) Accelerated in vitro fibril formation by a mutant alpha-synuclein linked to early-onset Parkinson disease. Nat Med 4(11):1318–1320, doi:10.1038/3311
15. Choi W, Zibaee S, Jakes R, Serpell LC, Davletov B, Crowther RA, Goedert M (2004) Mutation E46K increases phospholipid binding and assembly into filaments of human alpha-synuclein. FEBS Lett 576(3):363–368, doi:10.1016/j.febslet.2004.09.038
16. Ghosh D, Mondal M, Mohite GM, Singh PK, Ranjan P, Anoop A, Ghosh S, Jha NN, Kumar A, Maji SK (2013) The Parkinson's disease-associated H50Q mutation accelerates alpha-Synuclein aggregation in vitro. Biochemistry 52(40):6925–6927, doi:10.1021/bi400999d
17. Yonetani M, Nonaka T, Masuda M, Inukai Y, Oikawa T, Hisanaga S, Hasegawa M (2009) Conversion of wild-type alpha-synuclein into mutant-type fibrils and its propagation in the presence of A30P mutant. J Biol Chem 284 (12):7940–7950, doi:10.1074/jbc.M807482200
18. Braak H, Del Tredici K, Rub U, de Vos RA, Jansen Steur EN, Braak E (2003) Staging of brain pathology related to sporadic Parkinson's disease. Neurobiol Aging 24(2):197–211
19. Attems J, Walker L, Jellinger KA (2014) Olfactory bulb involvement in neurodegenerative diseases. Acta Neuropathol 127(4):459–475, doi:10.1007/s00401-014-1261-7
20. Luk KC, Kehm V, Carroll J, Zhang B, O'Brien P, Trojanowski JQ, Lee VM (2012) Pathological alpha-synuclein transmission initiates Parkinson-like neurodegeneration in nontransgenic mice. Science 338(6109):949–953, doi:10.1126/science.1227157
21. Masuda-Suzukake M, Nonaka T, Hosokawa M, Oikawa T, Arai T, Akiyama H, Mann DM, Hasegawa M (2013) Prion-like spreading of pathological alpha-synuclein in brain. Brain 136(Pt 4):1128–1138, doi:10.1093/brain/awt037
22. Mougenot AL, Nicot S, Bencsik A, Morignat E, Verchere J, Lakhdar L, Legastelois S, Baron T (2011) Prion-like acceleration of a synucleinopathy in a transgenic mouse model. Neurobiol Aging. doi:10.1016/j.neurobiolaging.2011.06.022
23. Luk KC, Kehm VM, Zhang B, O'Brien P, Trojanowski JQ, Lee VM (2012) Intracerebral inoculation of pathological alpha-synuclein initiates a rapidly progressive neurodegenerative alpha-synucleinopathy in mice. J Exp Med 209(5):975–986, doi:10.1084/jem.20112457
24. Watts JC, Giles K, Oehler A, Middleton L, Dexter DT, Gentleman SM, DeArmond SJ, Prusiner SB (2013) Transmission of multiple system atrophy prions to transgenic mice. Proc Natl Acad Sci U S A 110(48):19555–19560, doi:10.1073/pnas.1318268110
25. Recasens A, Dehay B, Bove J, Carballo-Carbajal I, Dovero S, Perez-Villalba A, Fernagut PO, Blesa J, Parent A, Perier C, Farinas I, Obeso JA, Bezard E, Vila M (2014) Lewy body extracts from Parkinson disease brains trigger alpha-synuclein pathology and neurodegeneration in mice and monkeys. Ann Neurol 75(3):351–362, doi:10.1002/ana.24066
26. Obi K, Akiyama H, Kondo H, Shimomura Y, Hasegawa M, Iwatsubo T, Mizuno Y, Mochizuki H (2008) Relationship of phosphorylated alpha-synuclein and tau accumulation to Abeta deposition in the cerebral cortex of dementia with Lewy bodies. Exp Neurol 210(2):409–420, doi:10.1016/j.expneurol.2007.11.019
27. Jakes R, Crowther RA, Lee VM, Trojanowski JQ, Iwatsubo T, Goedert M (1999) Epitope mapping of LB509, a monoclonal antibody directed against human alpha-synuclein. Neurosci Lett 269(1):13–16
28. Hasegawa M, Arai T, Nonaka T, Kametani F, Yoshida M, Hashizume Y, Beach TG, Buratti E, Baralle F, Morita M, Nakano I, Oda T, Tsuchiya K, Akiyama H (2008) Phosphorylated TDP-43 in frontotemporal lobar degeneration and amyotrophic lateral sclerosis. Ann Neurol 64(1):60–70, doi:10.1002/ana.21425
29. Abeliovich A, Schmitz Y, Farinas I, Choi-Lundberg D, Ho WH, Castillo PE, Shinsky N, Verdugo JM, Armanini M, Ryan A, Hynes M, Phillips H, Sulzer D, Rosenthal A (2000) Mice lacking alpha-synuclein display functional deficits in the nigrostriatal dopamine system. Neuron 25(1):239–252
30. Lee HJ, Gallagher M, Holland PC (2010) The central amygdala projection to the substantia nigra reflects prediction error information in appetitive conditioning. Learn Mem 17(10):531–538, doi:10.1101/lm.1889510
31. Smith AD, Bolam JP (1990) The neural network of the basal ganglia as revealed by the study of synaptic connections of identified neurones. Trends Neurosci 13(7):259–265
32. Gibb WR (1997) Functional neuropathology in Parkinson's disease. Eur Neurol 38(Suppl 2):21–25
33. Freundt EC, Maynard N, Clancy EK, Roy S, Bousset L, Sourigues Y, Covert M, Melki R, Kirkegaard K, Brahic M (2012) Neuron-to-neuron transmission of alpha-synuclein fibrils through axonal transport. Ann Neurol 72(4):517–524, doi:10.1002/ana.23747
34. Rey NL, Petit GH, Bousset L, Melki R, Brundin P (2013) Transfer of human alpha-synuclein from the olfactory bulb to interconnected brain regions in mice. Acta Neuropathol 126(4):555–573, doi:10.1007/s00401-013-1160-3
35. Ulusoy A, Rusconi R, Perez-Revuelta BI, Musgrove RE, Helwig M, Winzen-Reichert B, Di Monte DA (2013) Caudo-rostral brain spreading of alpha-synuclein through vagal connections. EMBO Mol Med 5(7):1051–1059, doi:10.1002/emmm.201302475
36. Braak H, Rub U, Gai WP, Del Tredici K (2003) Idiopathic Parkinson's disease: possible routes by which vulnerable neuronal types may be subject to neuroinvasion by an unknown pathogen. J Neural Transm 110(5):517–536, doi:10.1007/s00702-002-0808-2
37. Liu L, Drouet V, Wu JW, Witter MP, Small SA, Clelland C, Duff K (2012) Trans-synaptic spread of tau pathology in vivo. PLoS One 7(2):e31302, doi:10.1371/journal.pone.0031302
38. Iba M, Guo JL, McBride JD, Zhang B, Trojanowski JQ, Lee VM (2013) Synthetic tau fibrils mediate transmission of neurofibrillary tangles in a

transgenic mouse model of Alzheimer's-like tauopathy. J Neurosci 33(3):1024–1037, doi:10.1523/JNEUROSCI.2642-12.2013
39. Iseki E, Togo T, Suzuki K, Katsuse O, Marui W, de Silva R, Lees A, Yamamoto T, Kosaka K (2003) Dementia with Lewy bodies from the perspective of tauopathy. Acta Neuropathol 105(3):265–270, doi:10.1007/s00401-002-0644-3
40. Colom-Cadena M, Gelpi E, Charif S, Belbin O, Blesa R, Marti MJ, Clarimon J, Lleo A (2013) Confluence of alpha-synuclein, tau, and beta-amyloid pathologies in dementia with Lewy bodies. J Neuropathol Exp Neurol 72 (12):1203–1212, doi:10.1097/NEN.0000000000000018
41. Clinton LK, Blurton-Jones M, Myczek K, Trojanowski JQ, LaFerla FM (2010) Synergistic Interactions between Abeta, tau, and alpha-synuclein: acceleration of neuropathology and cognitive decline. J Neurosci 30(21):7281–7289, doi:10.1523/JNEUROSCI.0490-10.2010
42. Guo JL, Covell DJ, Daniels JP, Iba M, Stieber A, Zhang B, Riddle DM, Kwong LK, Xu Y, Trojanowski JQ, Lee VM (2013) Distinct alpha-synuclein strains differentially promote tau inclusions in neurons. Cell 154(1):103–117, doi:10.1016/j.cell.2013.05.057
43. Chung CY, Khurana V, Auluck PK, Tardiff DF, Mazzulli JR, Soldner F, Baru V, Lou Y, Freyzon Y, Cho S, Mungenast AE, Muffat J, Mitalipova M, Pluth MD, Jui NT, Schule B, Lippard SJ, Tsai LH, Krainc D, Buchwald SL, Jaenisch R, Lindquist S (2013) Identification and rescue of alpha-synuclein toxicity in Parkinson patient-derived neurons. Science 342(6161):983–987, doi:10.1126/science.1245296
44. Volpicelli-Daley LA, Luk KC, Patel TP, Tanik SA, Riddle DM, Stieber A, Meaney DF, Trojanowski JQ, Lee VM (2011) Exogenous alpha-synuclein fibrils induce Lewy body pathology leading to synaptic dysfunction and neuron death. Neuron 72(1):57–71, doi:10.1016/j.neuron.2011.08.033
45. Nonaka T, Watanabe ST, Iwatsubo T, Hasegawa M (2010) Seeded aggregation and toxicity of {alpha}-synuclein and tau: cellular models of neurodegenerative diseases. J Biol Chem 285(45):34885–34898, doi:10.1074/jbc.M110.148460

doi:10.1186/s40478-014-0088-8
Cite this article as: Masuda-Suzukake *et al.*: Pathological alpha-synuclein propagates through neural networks. *Acta Neuropathologica Communications* 2014 2:88.

Acta Neuropathol
DOI 10.1007/s00401-013-1191-9

CORRESPONDENCE

3R and 4R tau isoforms in paired helical filaments in Alzheimer's disease

Masato Hasegawa · Sayuri Watanabe · Hiromi Kondo · Haruhiko Akiyama · David M. A. Mann · Yuko Saito · Shigeo Murayama

Received: 20 August 2013 / Revised: 29 September 2013 / Accepted: 30 September 2013

Isoform-specific tau antibodies RD3 and RD4 are useful tools for investigating expression and localization of three-repeat (3R) and four-repeat (4R) tau isoforms. Recently, transition from 3R to 4R tau in Alzheimer's disease (AD) was proposed based on immunohistochemical studies with RD3 and RD4 [3]. Here, we show that two factors influence immunoreactivity to these antibodies. First, deamidation at the RD4 epitope abrogates immunoreactivity to RD4, and second, presentation of RD3 and RD4 epitopes is reciprocally affected by protease. Asparagine at position 279 in the RD4 epitope is predominantly deamidated to aspartic acid in pathological tau in AD brains [2, 4]. Consequently, the presence of 4R tau in AD pathologies may be underestimated when RD4 is used. However, anti-4R (available from Cosmo Bio Co., Ltd.) raised against RD4 peptide with N279D substitution stained both wild-type and deamidated 4R tau, and strongly stained RD3+/RD4− tangles and smearing tau fragments in Sarkosyl-insoluble fraction of AD brain [2].

It was reported that RD3 stained abundant ghost tangles in entorhinal cortex and tangles in CA1, but failed to stain fine processes of tangles and threads [3], while RD4 failed to detect ghost tangles in entorhinal cortex [3]. To understand these findings, we examined the influence of protease on immunoreactivity. Paraffin sections of AD brains were treated with 10 μg/mL Proteinase K (Pro-K) for 30 min after autoclaving (Ac) and formic acid (FA) treatment. RD3 staining was strongly enhanced (Fig. 1a, b). Conversely, RD4 immunoreactivity almost completely disappeared after Pro-K treatment (Fig. 1c, d). Not only ghost tangles but also RD3−/RD4+ tangles and their processes became RD3-positive after Pro-K treatment (Fig. 1a, b), strongly suggesting that the RD3 epitope was buried in tau filaments of intracellular tangles and threads, and was exposed by Pro-K treatment. Contrary to expectation, anti-4R staining was also enhanced by Pro-K treatment (Fig. 1e, f). It is possible that the recognition site of anti-4R is distinct from that of RD4 and is exposed by Pro-K treatment of sections. Anti-4R antibody may recognize the carboxyl-half of the antigen peptide, while RD4 recognizes the amino-terminal half around N279. Pro-K treatment was also effective in immunostaining of free-floating AD sections with a lower concentration.

To confirm these findings biochemically, Sarkosyl-insoluble fractions from two AD brains were treated with trypsin or Pro-K, then immunoblotted with RD3, RD4, anti-4R and anti-pS396 (Fig. 1g–j). RD3 strongly stained many bands and smears, as seen with pS396 (Fig. 1g, j),

M. Hasegawa (✉) · S. Watanabe
Department of Neuropathology and Cell Biology, Tokyo Metropolitan Institute of Medical Science, Setagaya-ku, Tokyo 156-8506, Japan
e-mail: hasegawa-ms@igakuken.or.jp

H. Kondo
Histology Center, Tokyo Metropolitan Institute of Medical Science, Setagaya-ku, Tokyo 156-8506, Japan

H. Akiyama
Dementia Research Project, Tokyo Metropolitan Institute of Medical Science, Setagaya-ku, Tokyo 156-8506, Japan

D. M. A. Mann
Centre for Clinical and Cognitive Neuroscience, Institute of Brain Behavior and Mental Health, University of Manchester, Salford M6 8HD, UK

Y. Saito
Department of Laboratory Medicine, National Center Hospital, NCNP, 4-1-1 Ogawahigashi, Kodaira, Tokyo 187-8502, Japan

S. Murayama
Department of Neuropathology, Tokyo Metropolitan Institute of Gerontology, Itabashi-ku, Tokyo 173-0015, Japan

Published online: 09 November 2013

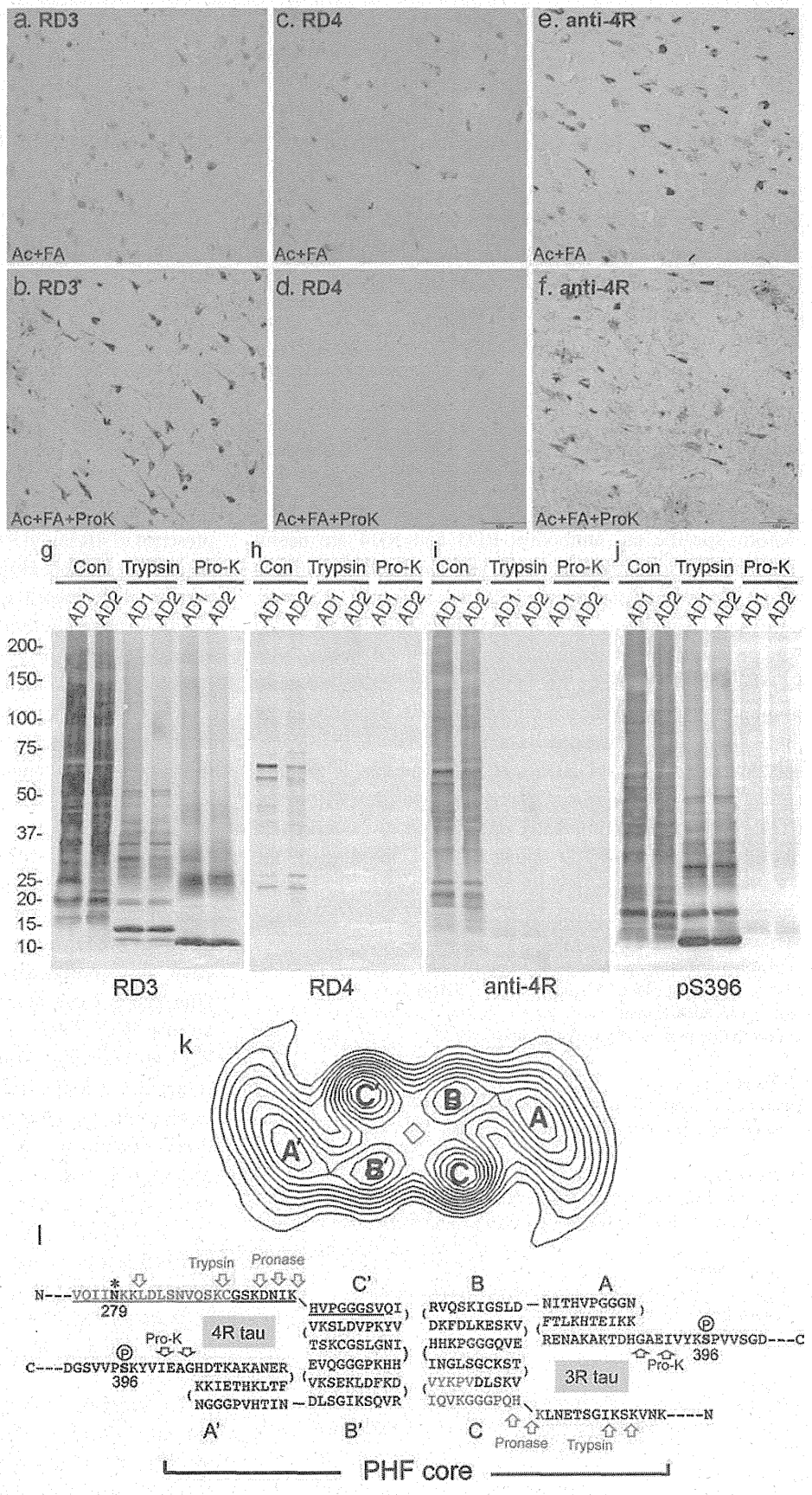

Fig. 1 **a–f** Immunostaining of AD sections after Ac and FA treatment before (**a**, **c**, **e**) and after (**b**, **d**, **f**) Pro-K treatment, using RD3 (**a**, **b**), RD4 (**c**, **d**) and anti-4R (**e**, **f**). *Bar* 100 μm. **g–j** Immunoblots of Sarkosyl-insoluble tau from two AD brains, before (*Con*) and after treatments with trypsin or Pro-K, using RD3 (**g**), RD4 (**h**), anti-4R (**i**) and pS396 (**j**). **k–l** Computed cross-section through a paired helical filament (**k**) [reproduced from Ref. [1], with permission of the publisher], a predicted folding model of 3R and 4R tau in PHF (**l**). RD3 and RD4 epitopes are indicated by *blue* and *red*, respectively. 4R tau specific insertion is indicated by *underlining*. The deamidation site N279 is indicated by *asterisks*. Phosphorylation of Ser396 is indicated. Possible trypsin, pronase and Pro-K cleavage sites are indicated in *green*, *purple* and *dark blue arrows*, respectively. The protease-resistant domain of PHF is indicated as *PHF-core*

whereas RD4 only labeled the 64/68 kDa doublet and some fragments at ~25 kDa (Fig. 1h). Anti-4R strongly stained the smears and fragments (Fig. 1i), suggesting that tau in these RD4-negative anti-4R-positive bands and smears is deamidated at N279. The weak RD4 and strong anti-4R immunoreactivities were completely abolished after trypsin or Pro-K treatment (Fig. 1h, i). This result is inconsistent with the immunohistochemistry, but protease sensitivity is likely different in fixed tissues. In contrast, the RD3 epitope was retained in the fragments, and RD3 strongly reacted with the protease-resistant 10–25 kDa bands after trypsin or Pro-K treatment (Fig. 1g). pS396 epitope was removed by Pro-K but not trypsin, suggesting a location outside the PHF core. Trypsin may not cleave the KSP site because of phosphorylation of Ser396. These results demonstrate reciprocal effects of protease treatment on RD3 and RD4 epitopes, indicating that RD4 epitope in tau in AD is susceptible to proteases, while RD3 epitope is highly resistant.

These results are consistent with previous findings. Wischik et al. identified two types of amino acid sequences, QPGGGKVQIVYK... (3R tau) and IKXVPGG... (4R tau), in 12-kDa tau fragment comprising the pronase-resistant core of PHFs [6] (see Fig. 1k). We identified HQPGGG... (3R tau) and HVPGGG... (4R tau) in 7–15 kDa trypsin-resistant fragments of PHF-tau in AD brains [5]. In both cases, 3R and 4R tau isoforms were detected, but the 4R tau N-terminus lacked the RD4 epitope. Based on these observations and a computed cross-section of PHF (Fig. 1k) [1], we propose a schematic model of tau folding in PHF (Fig. 1l). Analysis of the cross-sectional density in the PHF core on electron micrographs indicates the presence of two C-shaped morphological units, which correspond to the two strands of PHF, each with three domains (Fig. 1k) [1]. The RD3 epitope is buried in the PHF core and is normally masked by the N- or C-terminal region of tau, but is exposed in ghost tangles and/or in PHFs attacked by proteases. The RD4 epitope, which is mostly deamidated in PHF, is located slightly outside the core, where it can be digested by proteases (Fig. 1l). This model can explain the epitope masking of RD3 and RD4 and the reciprocal effects of degradation or protease treatment on the immunoreactivities.

This study indicates that differential presentation of epitopes can occur as a result of folding and processing, even when the epitopes are located in close proximity. Tau in PHFs appears to be processed gradually by intracellular proteases and more extensively in extracellular space during AD progression. We suggest that changes in immunoreactivity to antibodies reflect aging of tau in tangles or PHFs, which are composed of both 3R and 4R tau isoforms. We also show that Pro-K treatment of sections after Ac and FA treatment is useful for unmasking buried epitopes.

Acknowledgments We acknowledge the support of Alzheimer's Research UK and Alzheimer's Society through their funding of Manchester Brain Bank under the Brains for Dementia Research (BDR) initiative. This work was supported by Grants-in-Aid for Scientific Research (S) (JSPS KAKENHI 23228004), (A) (JSPS KAKENHI 23240050), and MHLW Grant 12946221 (to M.H.).

References

1. Crowther RA (1991) Straight and paired helical filaments in Alzheimer disease have a common structural unit. Proc Natl Acad Sci USA 88:2288–2292
2. Dan A, Takahashi M, Masuda-Suzukake M, Kametani F, Nonaka T, Kondo H, Akiyama H, Arai T, Mann DM, Saito Y, Hatsuta H, Murayama S, Hasegawa M (2013) Extensive deamidation at asparagine residue 279 accounts for weak immunoreactivity of tau with RD4 antibody in Alzheimer's disease brain. Acta Neuropathol Commun 1:54
3. Hara M, Hirokawa K, Kamei S, Uchihara T (2013) Isoform transition from four-repeat to three-repeat tau underlies dendrosomatic and regional progression of neurofibrillary pathology. Acta Neuropathol 125:565–579
4. Hasegawa M, Morishima-Kawashima M, Takio K, Suzuki M, Titani K, Ihara Y (1992) Protein sequence and mass spectrometric analyses of tau in the Alzheimer's disease brain. J Biol Chem 267:17047–17054
5. Hasegawa M, Watanabe A, Takio K, Suzuki M, Arai T, Titani K, Ihara Y (1993) Characterization of two distinct monoclonal antibodies to paired helical filaments: further evidence for fetal-type phosphorylation of the tau in paired helical filaments. J Neurochem 60:2068–2077
6. Wischik CM, Novak M, Thogersen HC, Edwards PC, Runswick MJ, Jakes R, Walker JE, Milstein C, Roth M, Klug A (1988) Isolation of a fragment of tau derived from the core of the paired helical filament of Alzheimer disease. Proc Natl Acad Sci USA 85:4506–4510